

X-RAY CRYSTALLOGRAPHIC ANALYSIS OF 2,5-BIS(DIPHENYLMETHYLSILYL)THIOPHENE MONOOXIDE AND THE DIELS-ALDER REACTION OF THIOPHENE MONOOXIDE WITH DIENOPHILES

Naomichi Furukawa,* Shao-Zhong Zhang, Ernst Horn, Ohgi Takahashi,
and Soichi Sato

*Tsukuba Advanced Research Alliance Center, and Department of Chemistry,
University of Tsukuba, Tsukuba, Ibaraki 305, Japan*

Masataka Yokoyama and Kentaro Yamaguchi

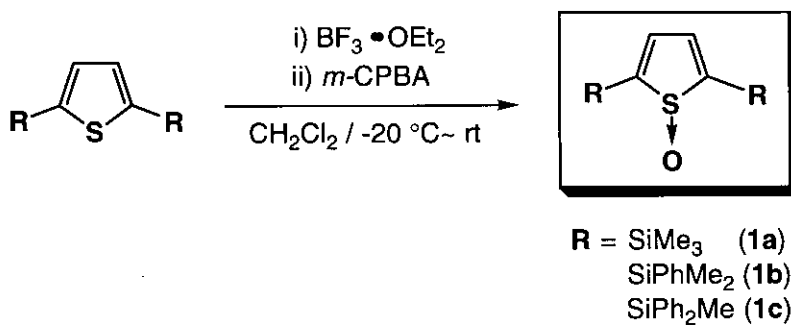
*Department of Chemistry, Chemical Analysis Center, Faculty of Science, Chiba
University, Chiba 263, Japan*

Abstract- X-Ray crystallographic analysis of 2,5-bis(diphenylmethylsilyl)thiophene monooxide revealed that the thiophene ring is not a planar structure and that the S–O bond is tilted *ca.* 14 ° out of the ring plane. The Diels-Alder reaction of 2,5-bis(trimethylsilyl)thiophene with dienophiles gave the adducts in high yields. The stereochemical courses for the reactions are exclusively *endo*-orientation and *syn*-direction with respect to the S–O bond. This stereochemistry agrees with the results obtained from RHF and MP2 MO calculations using the 6-31G(*) basis set.

Although the synthesis of a few thiophene monooxides has been reported, their chemical and physical properties have not been unraveled.¹ It is understood that for the preparation of the stable thiophene monooxides 2,5-bulky disubstituents² or prior complexation with the transition metals at the sulfur atom are required to prevent self-condensation of the monooxides.³ Although one uses bulky 2,5-disubstituted

thiophenes for oxidation, the corresponding thiophene dioxides⁴ are obtained more preferentially than the monooxides which are formed as by-products. This result suggests that the first oxidation step should be faster than that of the second step. In the course of our study of the oxidation reaction of thiophenes with *m*-chloroperbenzoic acid (*m*-CPBA), we found that the thiophene monooxides could be prepared in moderate yields when 2,5-bis(disilylated) thiophenes were oxidized with *m*-CPBA in the presence of $\text{BF}_3 \cdot \text{OEt}_2$ as shown in Scheme 1.⁵

Scheme 1



This reaction system may retard further oxidation of the monooxide to the dioxide. Furthermore, this procedure has been successfully applied for the synthesis of several 2,5-bisalkyl- and -phenylthiophenes by Tashiro *et al.*⁶ Thiophene monooxides generated *in situ* undergo the Diels-Alder reaction with dienophiles though no one has been able to isolate the monooxides during the reactions.^{6,7} As to the structure of thiophene monooxide, recently a X-Ray crystallographic analysis of 2,5-diphenylthiophene monooxide has been reported.⁸ In this paper, we wish to report the X-Ray crystallographic analysis of 2,5-bis(diphenylmethylsilyl)thiophene monooxide (**1c**) and the Diels-Alder reactions of 2,5-bis(trimethylsilyl)thiophene monooxide (**2**) with dienophiles, together with the stereochemical results and the *ab initio* calculation in the addition reactions.

Results and discussion

2,5-Bis(diphenylmethylsilyl)thiophene monooxide (**1c**) was prepared according to our preliminary reported procedure⁵ as shown in Scheme 1. The monooxide (**1c**) was isolated in 60% yield and purified by recrystallization repeatedly from chloroform.

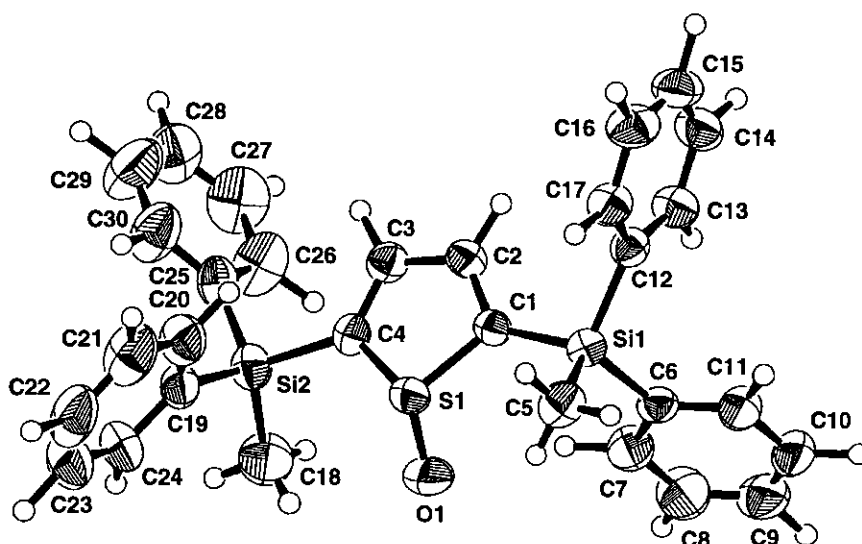


Figure 1. An ORTEP view of the thiophene monooxide (1c).

Table 1. Selected bond distances (Å) and angles (deg) with Esd's in parentheses for 1c^a

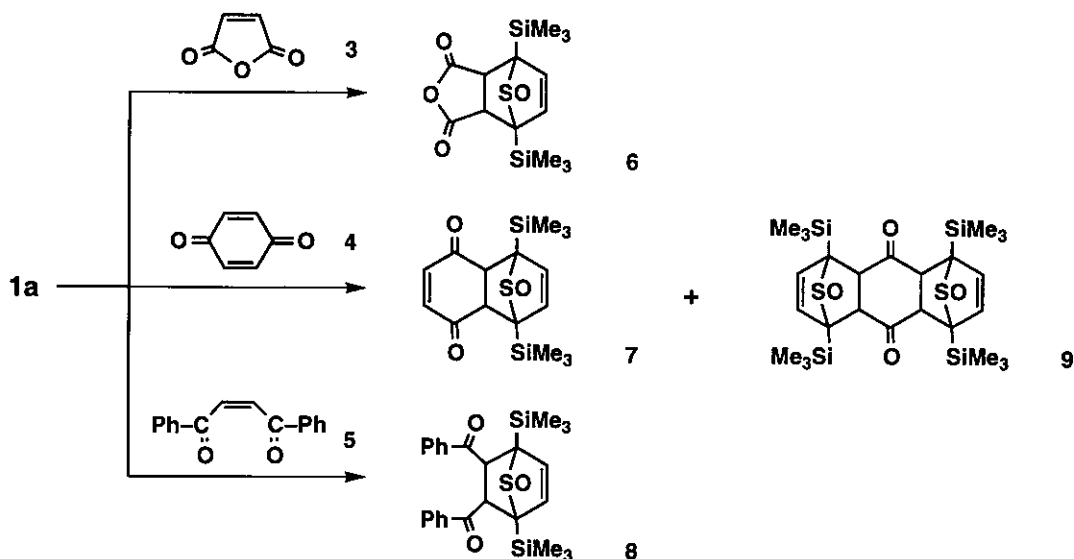
S(1)–O(1)	1.471(2)	S(1)–C(1)	1.764(2)	S(1)–C(4)	1.773(3)
Si(1)–C(1)	1.885(3)	Si(1)–C(5)	1.841(3)	Si(1)–C(6)	1.871(3)
Si(1)–C(12)	1.860(3)	Si(2)–C(4)	1.870(3)	Si(2)–C(18)	1.851(4)
Si(2)–C(19)	1.864(3)	Si(2)–C(25)	1.868(3)	C(1)–C(2)	1.341(3)
C(2)–C(3)	1.446(5)	C(3)–C(4)	1.346(4)	C(6)–C(3)	1.390(4)
O(1)–S(1)–C(1)	115.7(1)	O(1)–S(1)–C(4)	115.2(1)		
C(1)–S(1)–C(4)	94.4(1)	C(1)–Si(1)–C(5)	108.5(1)		
C(1)–Si(1)–C(6)	108.8(1)	C(1)–Si(1)–C(12)	104.8(1)		
C(5)–Si(1)–C(6)	111.7(1)	C(5)–Si(1)–C(12)	113.1(1)		
C(6)–Si(1)–C(12)	109.6(1)	C(4)–Si(2)–C(18)	109.7(2)		
C(4)–Si(2)–C(19)	108.2(1)	C(4)–Si(2)–C(25)	104.8(1)		
C(18)–Si(2)–C(19)	110.7(2)	C(18)–Si(2)–C(25)	111.2(2)		
C(19)–Si(2)–C(25)	112.0(1)	S(1)–C(1)–Si(1)	123.6(1)		
S(1)–C(1)–C(2)	106.6(2)	Si(1)–C(1)–C(2)	128.7(2)		
C(1)–C(2)–C(3)	115.4(2)	C(2)–C(3)–C(4)	115.2(2)		
S(1)–C(4)–Si(2)	123.4(1)	S(1)–C(4)–C(3)	106.3(2)		
Si(2)–C(4)–C(3)	129.8(2)	Si(1)–C(6)–C(7)	121.9(2)		

^a Numbers in parentheses are estimated standard deviations in the least significant digits.

The physical properties of **1c** are identical with those reported before. The structure of **1c** was finally determined by X-Ray crystallographic analysis. An ORTEP drawing, and the corresponding bond distances and angles are presented in Figure 1 and Table 1.

As shown in Figure 1, the structure of monooxide (**1c**) is a half envelop and the S–O bond is tilted *ca.* 13.6° out of the four carbon thiophene ring plane. The S–O bond length is 1.472 Å which is almost identical value of that of 2,5-diphenyl derivative.⁸ The C–C bond lengths between C2=C3, C3–C4 bonds are 1.345 and 1.448 Å, respectively, indicating that the structure of **1c** is a typical diene form with a similar structure to that of the 2,5-diphenyl derivative and the dioxide reported earlier.⁴ This structural analysis of monooxide (**1c**) suggests that the monooxides should serve as dienes and undergo the Diels-Alder addition reaction with dienophiles. For simplicity, we used the 2,5-bis(trimethylsilyl)thiophene monooxide (**1a**) as a representative diene analog for the [4 + 2] addition reaction.

Scheme 2



As dienophiles, the following three compounds, maleic anhydride (**3**), benzoquinone (**4**) and *cis*-1,2-dibenzoylene (**5**) were used for performance of the addition reactions. Whereas the acetylene derivatives, *trans*-1,2-dibenzoylene did not react with **1a** at the same reaction conditions. The addition reactions were carried out using one equivalent of each of the monooxide (**1a**) and the diene in CH₂Cl₂ at 0

– 5 °C. The reactions proceeded cleanly to give the [4 + 2] adducts in highly regio- and stereo-selective manners. The products were separated and purified by liquid chromatography. The spectroscopic results suggest that their structures of the products (6) – (8) are as shown in Scheme 2.

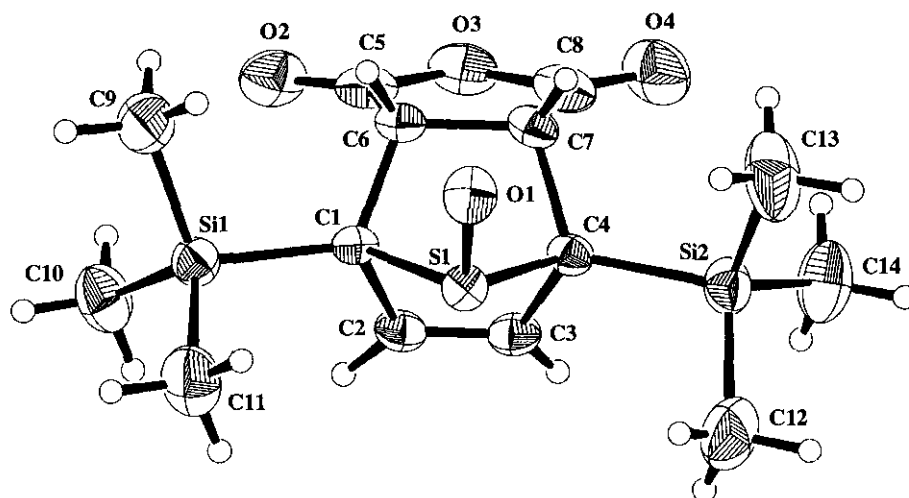


Figure 2. An ORTEP view of 6.

Table 2. Selected bond distances (Å) and angles (deg) with Esd's in parentheses for 6^a

S(1)–O(1)	1.490(3)	S(1)–C(1)	1.858(4)	S(1)–C(4)	1.861(4)
Si(1)–C(1)	1.905(4)	Si(2)–C(4)	1.901(4)	O(2)–C(5)	1.176(5)
O(3)–C(5)	1.374(5)	O(3)–C(8)	1.407(6)	O(4)–C(8)	1.177(5)
C(1)–C(2)	1.525(5)	C(1)–C(6)	1.553(5)	C(2)–C(3)	1.317(6)
C(3)–C(4)	1.521(5)	C(4)–C(7)	1.560(5)	C(5)–C(6)	1.492(6)
C(6)–C(7)	1.531(6)	C(7)–C(8)	1.490(6)		
O(1)–S(1)–C(1)	108.8(2)	O(1)–S(1)–C(4)	109.6(2)		
C(1)–S(1)–C(4)	83.9(2)	C(1)–Si(1)–C(9)	108.9(2)		
C(4)–Si(2)–C(12)	107.2(2)	C(5)–O(3)–C(8)	110.5(3)		
S(1)–C(1)–C(2)	94.4(2)	S(1)–C(1)–C(6)	100.1(2)		
C(2)–C(1)–C(6)	107.7(3)	C(1)–C(2)–C(3)	112.5(3)		
S(1)–C(4)–Si(2)	112.8(2)	S(1)–C(4)–C(3)	94.6(2)		
S(1)–C(4)–C(7)	99.6(2)	O(3)–C(5)–C(6)	110.6(4)		
C(1)–C(6)–C(5)	112.2(3)	C(1)–C(6)–C(7)	108.1(3)		
C(5)–C(6)–C(7)	104.4(4)	O(3)–C(8)–O(4)	119.4(5)		

^a Numbers in parentheses are estimated standard deviations in the least significant digits.

The structures of the products (6) – (8) were subsequently identified by X-Ray crystallographic analysis and their ORTEP drawings are shown in Figures 2, 3, and 4, respectively.

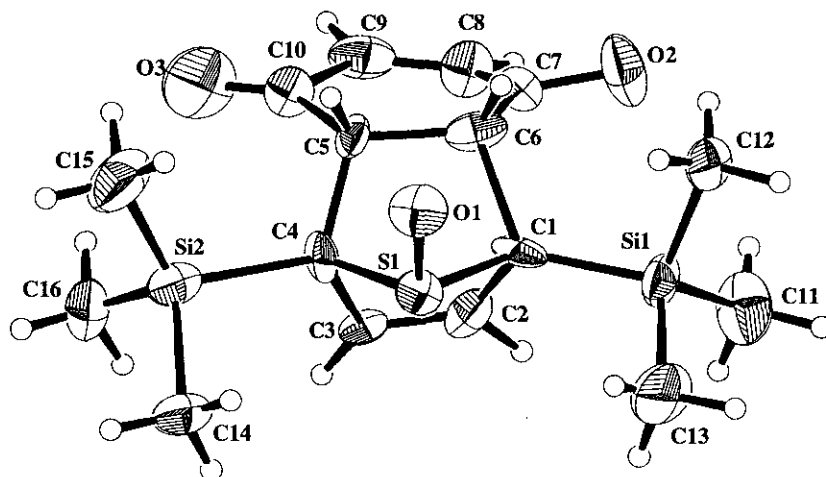


Figure 3. An ORTEP view of 7.

Table 3. Selected bond distances (Å) and angles (deg) with Esd's in parentheses for 7^a

S(1)–O(1)	1.485(5)	S(1)–C(1)	1.86(2)	S(1)–C(4)	1.82(2)
Si(1)–C(1)	1.85(2)	Si(2)–C(4)	1.95(2)	O(2)–C(7)	1.31(3)
O(3)–C(10)	1.12(3)	C(1)–C(2)	1.42(3)	C(1)–C(6)	1.62(2)
C(2)–C(3)	1.34(1)	C(3)–C(4)	1.51(2)	C(4)–C(5)	1.57(3)
C(5)–C(6)	1.55(1)	C(5)–C(10)	1.53(3)	C(6)–C(7)	1.53(3)
C(7)–C(8)	1.27(4)	C(8)–C(9)	1.32(1)	C(9)–C(10)	1.62(4)
O(1)–S(1)–C(1)	109.1(8)	C(1)–S(1)–C(4)	84.7(4)		
C(1)–Si(1)–C(11)	108(1)	S(1)–C(1)–Si(1)	113(1)		
S(1)–C(1)–C(2)	92(1)	S(1)–C(1)–C(6)	98(1)		
Si(1)–C(1)–C(2)	121(1)	Si(1)–C(1)–C(6)	122(1)		
C(2)–C(1)–C(6)	102(1)	C(1)–C(2)–C(3)	124(2)		
C(2)–C(3)–C(4)	102(1)	C(4)–C(5)–C(6)	106(1)		
C(6)–C(5)–C(10)	118(2)	C(1)–C(6)–C(5)	106(2)		
C(1)–C(6)–C(7)	111(1)	C(5)–C(6)–C(7)	113(1)		
O(2)–C(7)–C(6)	111(2)	O(2)–C(7)–C(8)	121(2)		
C(6)–C(7)–C(8)	127(2)	C(7)–C(8)–C(9)	122(3)		

^a Numbers in parentheses are estimated standard deviations in the least significant digits.

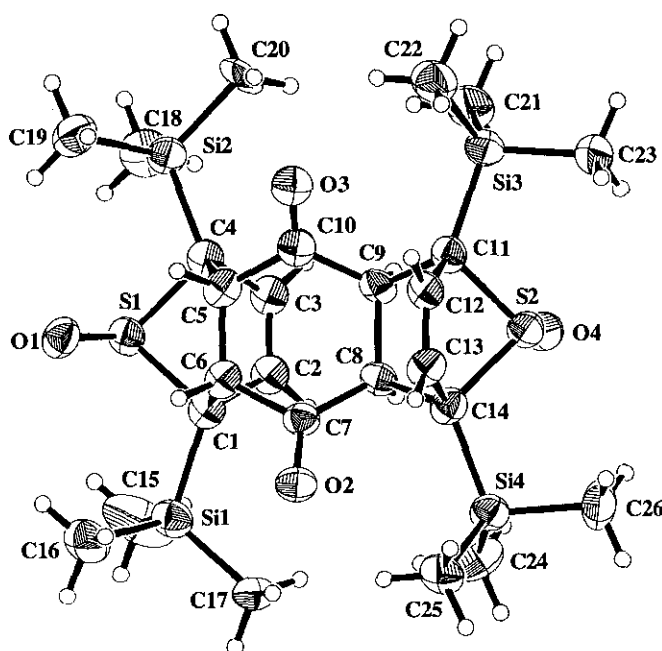


Figure 4. An ORTEP view of 9.

Table 4. Selected bond distances (Å) and angles (deg) with Esd's in parentheses for 9^a

O(1)–O(1)	1.490(7)	S(1)–C(1)	1.857(9)	S(1)–C(4)	1.89(1)
S(2)–O(4)	1.513(6)	Si(1)–C(1)	1.90(1)	O(2)–C(7)	1.23(1)
C(1)–C(2)	1.52(2)	C(1)–C(6)	1.590(10)	C(2)–C(3)	1.32(1)
C(5)–C(6)	1.52(1)	C(6)–C(7)	1.54(1)	C(7)–C(8)	1.47(2)
C(8)–C(9)	1.54(1)	C(8)–C(14)	1.58(1)	C(11)–C(12)	1.56(1)
C(12)–C(13)	1.28(1)	C(13)–C(14)	1.54(1)	S(2)–C(14)	1.86(1)
O(1)–S(1)–C(1)	109.7(4)	C(1)–S(1)–C(4)	83.9(5)		
O(4)–S(2)–C(11)	109.9(3)	O(4)–S(2)–C(14)	109.8(4)		
C(11)–S(2)–C(14)	86.1(5)	S(1)–C(1)–C(2)	95.3(6)		
S(1)–C(1)–C(6)	98.7(5)	C(2)–C(1)–C(6)	109.2(9)		
C(1)–C(2)–C(3)	112.5(8)	C(1)–C(6)–C(7)	110.1(6)		
C(5)–C(6)–C(7)	115.2(9)	O(2)–C(7)–C(6)	118(1)		
C(6)–C(7)–C(8)	118.8(10)	C(7)–C(8)–C(14)	113.6(8)		
S(2)–C(11)–C(9)	100.1(6)	S(2)–C(14)–C(8)	99.6(7)		
S(2)–C(14)–C(13)	94.7(7)	C(8)–C(14)–C(13)	105.1(7)		

^a Numbers in parentheses are estimated standard deviations in the least significant digits.

The crude products from the reactions in NMR tubes also showed the formation of **6** – **9** as single stereoisomers.

The stereochemical courses of these [4 + 2] addition reactions demonstrate clearly that the addition proceeds in an *endo*-direction and the dienes approach from the *syn*-side to the S–O bond of **1a**. In the case of the reaction shown in Scheme 2, when two equivalents of monooxide (**1a**) were added to one equivalent of the diene (**5**), the major product obtained was the bis-adduct (**9**). In contrast to the dienes (**3**) – (**5**), the *trans*-diene and acetylenic compound (**10**) did not react at all with **1a** under the same reaction conditions due probably to the steric reasons. The *syn*-addition mode of the reactions was also confirmed by *ab initio* calculations for the Diels–Alder reaction of thiophene monooxide and ethylene. The calculations were carried out at the RHF and MP2 levels with the 6-31G* basis set.⁹ The RHF and MP2 calculations were carried out using Spartan 4.1¹⁰ and Gaussian 94,¹¹ respectively. The calculated relative energies of the

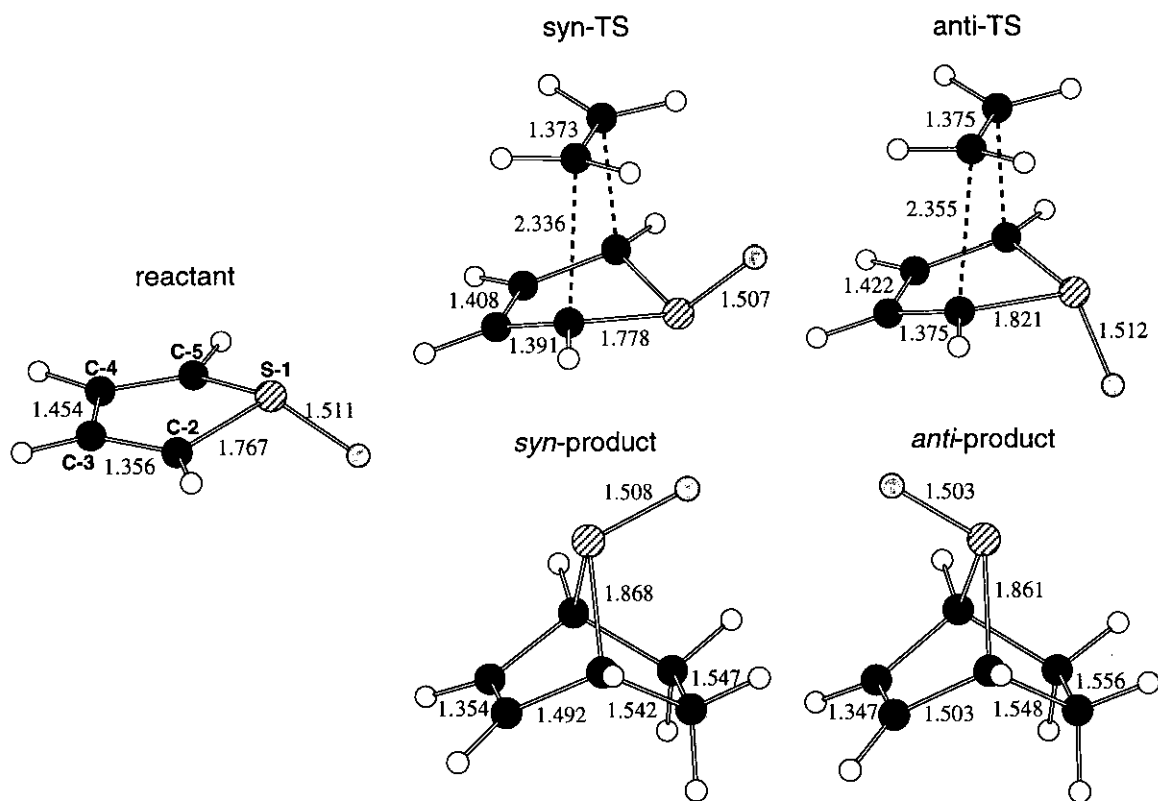


Figure 5. MP2/6-31G* geometries of thiophene monooxide, syn and anti transition states, and *syn* and *anti* products. The values are skeletal bond lengths in Å. All geometries have C_s symmetry.

reactant, *syn* and *anti* transition states (TS), and *syn* and *anti* products are shown in Table 5. The MP2 geometries for each stationary points are shown in Figure 5.

The activation barriers are drastically reduced and the exothermicity is largely increased by inclusion of electron correlation. Note that the calculated activation barriers and exothermicity of the Diels–Alder reaction of butadiene and ethylene are strongly method-dependent.¹² Anyway, however, the present calculations show that the *syn*-addition is much more favored than the *anti*-addition both kinetically and thermodynamically. The barrier for *syn*-addition is about 9 kcal•mol^{−1} lower than that for *anti*-addition. The activation barriers calculated at the RHF level are similar to those calculated for the Diels–Alder reaction of 2,5-dimethylthiophene oxide and maleic anhydride using semi-empirical calculations.¹³

The *syn*- π -facial selectivity is explained by the orbital mixing rule¹⁴ in the same manner as for the 5-substituted 1,3-cyclopentadienes. The π -HOMO of the diene part is modified by an out-of-phase combination with the low-lying n-orbital of the oxygen atom to become the HOMO of the whole molecule. The π -HOMO is further mixed with σ -orbitals in such a way that σ and n are out of phase. As a result, the HOMO is distorted so as to favor the *syn*-addition. The calculated HOMO is indeed distorted in such a way.

Though the facial selectivity is explained by the orbital mixing rule in this way, we would like to stress that the carbon atoms at the reaction centers, C-2 and C-5, of the thiophene monooxide molecule are already distorted from planarity so as to conform to the *syn*-addition. The sulfur atom protrudes out of the diene plane in the opposite direction to the oxygen atom, while the hydrogen atoms attached to C-2 and C-5 lie almost in the diene plane. The (C-4)–(C-5)–(C-2)–(S-1) dihedral angle is calculated to be 9.0° and 13.2° by the RHF/6-31G* and MP2/6-31G* methods, respectively.

Table 5. Calculated energies (kcal•mol^{−1}) of transition states and products relative to the reactant (thiophene monooxide + ethylene) (the values in parentheses are zero-point vibration energy corrections)

stationary point	RHF/6-31G*	MP2/6-31G*
<i>syn</i> -TS	30.7 (+2.4)	1.4 (+2.1)
<i>anti</i> -TS	39.6 (+2.2)	10.8 (+1.8)
<i>syn</i> -product	−38.5 (+6.2)	−53.2 (+6.1)
<i>anti</i> -product	−31.4 (+6.0)	−45.1 (+5.9)

Additional crystallographic details and tables of crystal data, positional parameters, thermal parameters, bond distances and angles have been deposited at Cambridge Crystallographic Data Center.

EXPERIMENTAL SECTION

General Data

All melting points were uncorrected and were taken on a Laboratory Devices Mel-Temp II and a Yanaco micromelting point apparatus. All NMR spectra were measured on a JEOL LMN-EX-270 or a Bruker ARX-400 spectrometer. Mass spectra were taken with a Shimadzu QP-2000 and a JEOL JMX SX102 mass spectrometer. Elemental analyses were carried out by the Chemical Analysis Center at the University of Tsukuba.

All reagents were obtained from Wako Pure Chemical Industries Ltd., Tokyo Kasei Co. Ltd., or Aldrich Chemical Co. The reagents used as reaction solvents were further purified by general methods.

Preparations

2,5-Bis(trimethylsilyl)thiophene Monooxide (1a). Boron trifluoride-etherate $\text{BF}_3 \cdot \text{OEt}_2$ (0.19 mL, 1.5 mmol) was added to a solution of 2,5-bis(trimethylsilyl)thiophene (114 mg, 0.5 mmol) in dry CH_2Cl_2 (4 mL) at -20°C under an argon atmosphere, and *m*-CPBA (104 mg, 0.6 mmol) in dry CH_2Cl_2 (2 mL) was added to the solution. The reaction was monitored occasionally by TLC analysis on silica gel. After the reaction, saturated aqueous sodium carbonate was added to the reaction mixture, and the organic layer was extracted with chloroform (3 x 50 mL). The combined organic layer was washed with brine (3 x 50 mL) and dried over anhydrous sodium sulfate. After removal of the solvent, the residue was subjected to column chromatography on silica gel (hexane : ethyl acetate = 3 : 1 v/v) to afford the monooxide (**1a**). Recrystallization from hexane gave colorless crystals (50 mg, 62%). mp 128°C ; ^1H NMR (270 MHz, CDCl_3 , rt) δ 0.35 (s, 18H, Me), 6.82 (s, 2H, Th-H); ^{13}C NMR (68 MHz, CDCl_3 , rt) δ 0.8, 137.9, 161.5; MS (*m/z*) 244 (M^+); IR (KBr, cm^{-1}) 1048 (S-O); Anal. Calcd for $\text{C}_{10}\text{H}_{20}\text{OSSi}_2$ C; 49.12, H; 8.24. Found C; 48.96, H; 8.61.

2,5-Bis(dimethylphenylsilyl)thiophene Monooxide (1b). Boron trifluoride-etherate $\text{BF}_3 \cdot \text{OEt}_2$ (6.2 mL, 50 mmol) was added to a solution of 2,5-bis(dimethylphenylsilyl)thiophene (1.76 g, 5.0 mmol) in dry CH_2Cl_2 (50 mL) at -20°C under an argon atmosphere, and *m*-CPBA (863 mg, 5.0 mmol) in dry CH_2Cl_2 (50 mL) was added to the solution. The reaction was monitored occasionally by TLC analysis on silica gel. After the reaction, saturated aqueous sodium carbonate was added to the reaction mixture, and

the organic layer was extracted with CH_2Cl_2 (3 x 80 mL). The combined organic layer was washed with brine (3 x 50 mL) and dried over anhydrous magnesium sulfate. After removal of the solvent, the residue was subjected to column chromatography on silica gel (hexane : ethyl acetate = 3 : 1 v/v) to afford the monooxide (**1b**). Recrystallization from hexane gave colorless crystals (829 mg, 45%). mp 73–74 °C; ^1H NMR (270 MHz, CDCl_3 , rt) δ 0.64 (s, 12H, Me), 6.71 (s, 2H, Th-H), 7.38–7.40 (m, 6H, Ph-H), 7.58–7.61 (m, 4H, Ph-H); ^{13}C NMR (68 MHz, CDCl_3 , rt) δ –2.5, 128.1, 129.8, 133.9, 135.8, 137.7, 158.8; MS (m/z) 368 (M^+); IR (KBr, cm^{-1}) 1046 (S–O); Anal. Calcd for $\text{C}_{20}\text{H}_{24}\text{OSSi}_2$ C; 65.16, H; 6.56. Found C; 64.89, H; 6.45.

2,5-Bis(diphenylmethylsilyl)thiophene Monooxide (1c). Boron trifluoride-etherate $\text{BF}_3 \cdot \text{OEt}_2$ (15.4 mL, 125 mmol) was added to a solution of 2,5-bis(diphenylmethylsilyl)thiophene (2.38 g, 5.0 mmol) in dry CH_2Cl_2 (80 mL) at –20 °C under an argon atmosphere, and *m*-CPBA (863 mg, 5.0 mmol) in dry CH_2Cl_2 (50 mL) was added to the solution. The reaction was monitored occasionally by TLC analysis on silica gel. After the reaction, saturated aqueous sodium carbonate was added to the reaction mixture, and the organic layer was extracted with CH_2Cl_2 (3 x 80 mL). The combined organic layer was washed with brine (3 x 50 mL) and dried over anhydrous magnesium sulfate. After removal of the solvent, the residue was subjected to column chromatography on silica gel (hexane : ethyl acetate = 3 : 1 v/v) to afford the monooxide (**1c**). Recrystallization from hexane gave colorless crystals (370 mg, 15%). mp 157 °C; ^1H NMR (270 MHz, CDCl_3 , rt) δ 0.93 (s, 6H, Me), 6.76 (s, 2H, Th-H), 7.34–7.37 (m, 12H, Ph-H), 7.54–7.56 (m, 8H, Ph-H); ^{13}C NMR (68 MHz, CDCl_3 , rt) δ –3.61, 128.1, 130.0, 134.0, 135.0, 139.4, 158.1; MS (m/z) 492 (M^+); IR (KBr, cm^{-1}) 1058 (S–O); Anal. Calcd for $\text{C}_{30}\text{H}_{28}\text{OSSi}_2$ C; 73.12, H; 5.73. Found C; 72.69, H; 5.63.

Diels-Alder Reaction of the Thiophene Monooxide (1a) with Maleic Anhydride (3). To a solution of thiophene monooxide (**1a**) (756 mg, 3.1 mmol) in dry CH_2Cl_2 (20 mL) was added dropwise a solution of maleic anhydride (294 mg, 3.0 mmol) in dry CH_2Cl_2 (20 mL) at 0 °C under an argon atmosphere. After removal of the solvent at rt, the residue was subjected to column chromatography on silica gel (CH_2Cl_2) to give the corresponding Diels-Alder reaction products (**6**). Recrystallization from CH_2Cl_2 : EtOH (10 : 1 v/v) gave colorless crystals (**6**; 1.02 g, 99%). mp 200–201 °C (decomp); ^1H NMR (400 MHz, CDCl_3 , rt) δ 0.34 (s, 18H, Me), 4.37 (s, 2H, Olefin-H), 6.31 (s, 2H, Th-H); ^{13}C NMR (100

MHz, CDCl_3 , rt) δ -2.56, 50.4, 67.4, 133.3, 169.7; MS (m/z) 342 (M^+); IR (KBr, cm^{-1}) 1785 ($\text{C}=\text{O}$); Anal. Calcd for $\text{C}_{14}\text{H}_{22}\text{O}_4\text{SSi}_2$ C; 49.09, H; 6.47. Found C; 49.05, H; 6.54.

Diels-Alder Reaction of the Thiophene Monooxide (1a) with Benzoquinone (4). A dry CH_2Cl_2 (20 mL) solution of thiophene monooxide (**1a**) (732 mg, 3.0 mmol) was added dropwise to a dry CH_2Cl_2 (20 mL) solution of benzoquinone (**4**) (335 mg, 3.1 mmol) at rt under an argon atmosphere. After removal of the solvent at rt, the residue was subjected to column chromatography on silica gel (CH_2Cl_2) to give the corresponding Diels-Alder reaction products (**7**) and (**9**). Recrystallization from CH_2Cl_2 : EtOH (10 : 1 v/v) gave yellow crystals (**7**; 994 mg, 94% and **9**; 36 mg, 4%). On the other hand, the reaction of **1a** (756 mg, 3.1 mmol) in dry CH_2Cl_2 (20 mL) with **4** (162 mg, 1.5 mmol) in CH_2Cl_2 (40 mL) under same condition afforded the corresponding Diels-Alder reaction products (**7**; 227 mg, 43% and **9**; 510 mg, 57%) as colorless crystals. **7**: mp 160 °C (decomp); ^1H NMR (270 MHz, CDCl_3 , rt) δ 0.31 (s, 18H, Me), 4.11 (s, 2H, Queno-H), 6.13 (s, 2H, Th-H), 6.68 (s, 2H, Queno-H); ^{13}C NMR (68 MHz, CDCl_3 , rt) δ -1.53, 50.5, 69.1, 133.8, 142.6, 198.0; MS m/z 352 (M^+); IR (KBr, cm^{-1}) 1069 (S-O) 1673 ($\text{C}=\text{O}$); Anal. Calcd for $\text{C}_{16}\text{H}_{24}\text{O}_3\text{SSi}_2$ C; 54.50, H; 6.86. Found C; 54.25, H; 6.73. **9**: mp 231–232 °C (decomp); ^1H NMR (270 MHz, CDCl_3 , rt) δ 0.26 (s, 36H, Me), 3.82 (s, 4H, Queno-H), 6.31 (s, 4H, Th-H); ^{13}C NMR (100 MHz, CDCl_3 , rt) δ -1.5, 57.3, 68.3, 134.0, 208.3; MS m/z 596 (M^+); IR (KBr, cm^{-1}) 1079 (S-O), 1702 ($\text{C}=\text{O}$); Anal. Calcd for $\text{C}_{26}\text{H}_{44}\text{O}_4\text{S}_2\text{Si}_4$ C; 52.30, H; 7.43. Found C; 52.33, H; 7.51.

Diels-Alder Reaction of the Thiophene Monooxide (1a) with *cis*-1,2-Dibenzoylethylene (5). A dry CHCl_3 (50 mL) solution of thiophene monooxide (**1a**) (3.0 mmol, 756 mg) was added dropwise to dry CHCl_3 (50 mL) solution of dienophile reagent (**5**) (851 mg, 3.6 mmol) for two weeks at 50 °C under an argon atmosphere. After removal of the solvent at rt, the residue was subjected to column chromatography on silica gel (CH_2Cl_2) to give the corresponding Diels-Alder reaction products (**8**), quantitatively. Recrystallization from CH_2Cl_2 : EtOH (10 : 1 v/v) gave colorless crystals (**8**; 1.30 g, 90%). mp 203 °C (decomp); ^1H NMR (270 MHz, CDCl_3 , rt) δ 0.16 (s, 18H, Me), 5.36 (s, 2H), 6.36 (s, 2H, Th-H), 7.17 (t, J = 7.3 Hz, 4H, Ar-H), 7.30 (t, J = 7.3 Hz, 2H, Ar-H), 7.73 (d, J = 7.3 Hz, 2H, Ar-H); ^{13}C NMR (100 MHz, CDCl_3 , rt) δ -1.8, 54.9, 68.0, 128.0, 132.1, 133.0, 137.6, 198.2; MS m/z 480

(M⁺); IR (KBr, cm⁻¹) 1064 (S–O); Anal. Calcd for C₂₆H₃₂O₃SSi₂ C; 64.95, H; 6.71. Found C; 65.02, H; 6.67.

Crystal Structure Determinations of 1b, 6, 7, and 9. X-Ray data for **1b**, **6** and **7** were collected on an Enraf-Nonius CAD4-FR four-circle diffractometer and the data for **9** were measurement on a Rigaku RAXIS II imaging plate area detector. The crystallographic details are given in Table 5. All structures were solved by direct methods,¹⁵ expanded using difference Fourier syntheses and refined on *F*² by full-matrix least-squares techniques. All non-carbon and non-hydrogen atoms were modeled anisotropically and the rest isotropically using neutral atom scattering factors. The absolute structure of **7** was determined by the atomic coordinates inversion method.¹⁶ The neutral atom scattering factors used in the refinements were taken from Cromer and Waber¹⁷ and corrected for anomalous dispersion¹⁸ using the *f'* and *f''* values determined by Creagh and McAuley.¹⁹ The teXsan²⁰ crystallographic software package was used for the refinement and geometrical calculations, and molecular graphics. All calculations were done on a Indy work station.

(i) Compound (1b). Data were collected for a colorless prismatic crystal mounted on top of a glass fiber. Unit cell parameters were determined from a least-square treatment of the SET4 setting angles of 25 reflections in the range 11.00 < 2θ < 20.0°. The intensities of 7063 reflections were corrected for Lp effects, absorption (DIFABS²¹, correction range 0.60 – 1.00), extinction (coefficient = 6.68310e-07) and crystal decay (1.3%). In the final cycle of full-matrix least-squares all non-hydrogen atoms were refined anisotropically. The hydrogen atoms were added to the respective carbon atoms at calculated positions (C–H: phenyl and methyl distances 1.08 and 0.97 Å) and subsequently their coordinates were refined but their isotropic B's were fixed. The remaining maximum and minimum electron density features in the final difference Fourier map are equal to 1.02 and –0.50 e/Å³, respectively.

(ii) Compound (6). Data were collected for a colorless prismatic crystal glued to the top of a glass fiber. Unit cell parameters were determined from a least-square treatment of the SET4 setting angles of 25 reflections in the range 8.00 < 2θ < 18.0°. The intensities of 5744 reflections were corrected for Lp effects, absorption (DIFABS²¹, correction range 0.49 – 1.00) and crystal decay (6.2%). In the final cycle of full-matrix least-squares all non-hydrogen atoms were refined anisotropically. The hydrogen atoms were added to the respective carbon atoms at calculated positions (C–H: phenyl and methyl distances 1.08 and 0.97 Å) and subsequently the coordinates of the non-methyl hydrogen atoms were refined but their isotropic B's were fixed, while the others were fixed during the refinement. The remaining maximum and

minimum electron density features in the final difference Fourier map are equal to 0.29 and $-0.32 \text{ e}/\text{\AA}^3$, respectively.

Table 5. X-Ray Crystallographic Data of the Structure Determination of **1b**, **6**, **7**, and **9**

compd	1b	6	7	9
formula	$\text{C}_{30}\text{H}_{28}\text{OSSi}_2$	$\text{C}_{14}\text{H}_{22}\text{O}_4\text{SSi}_2$	$\text{C}_{16}\text{H}_{24}\text{O}_3\text{SSi}_2$	$\text{C}_{26}\text{H}_{44}\text{O}_4\text{S}_2\text{Si}_4$
fw	492.78	707.56	352.59	597.09
cryst syst	monoclinic	monoclinic	orthorhombic	triclinic
space group	$P2_1/c$ (No. 14)	$C2/c$ (No. 15)	$P2_12_12_1$ (No. 19)	$P(\bar{1})$ (No. 2)
a , Å	14.187(3)	27.212(2)	6.880(1)	14.55(2)
b , Å	10.423(1)	8.627(1)	13.255(2)	17.085(6)
c , Å	19.161(5)	20.267(2)	20.787(3)	6.730(4)
α , deg	90.00(0)	90.00(0)	90.00(0)	100.22(3)
β , deg	105.82(1)	130.31(1)	90.00(0)	99.41(9)
γ , deg	90.00(0)	90.00(0)	90.00(0)	85.84(7)
V , Å ³	2726.2(8)	3627.8(8)	1895.7(4)	1622(1)
Z	4	8	4	2
D_{calcd} , g cm ⁻³	1.20	1.25	1.24	1.22
$F(000)$	1040.0	1456.0	752.0	640.0
temp, °C	23±1	23±1	23±1	15±1
radiation (λ , Å)	Mo K α (0.710 73)	Mo K α (0.710 73)	Mo K α (0.710 73)	Mo K α (0.710 73)
cryst dims, mm	0.60 x 1.00 x 1.10	0.45 x 0.70 x 1.20	0.25 x 0.70 x 0.80	0.30 x 0.50 x 0.65
m , cm ⁻¹	12.5	3.21	3.05	3.40
scan type	ω -2 θ	ω -2 θ	ω -2 θ	imaging plate (46 images)
scan rate	2–20 deg/min	2–20 deg/min	2–20 deg/min	6.0 min. exp./image
scan width, deg	$0.7 + 0.35 \tan \theta$	$0.7 + 0.41 \tan \theta$	$1.0 + 0.51 \tan \theta$	
Maxi 2 θ , deg	56.0	60.0	60.0	44.0
tot no. of rflns	7063	5744	6166	2190
no. of unique rflns	6871	5603	3159	2068
no. of params	392	202	199	326
refined				
rflns included	3976 ($I > 5\sigma(I)$)	2376 ($I > 5\sigma(I)$)	1000 ($I > 3\sigma(I)$)	2068 ($I > 3\sigma(I)$)
agreement factors ^a				
R	0.047	0.048	0.045	0.069
R_w	0.045	0.051	0.043	0.077

^a $R = \Sigma ||F_o| - |F_c|| / \Sigma |F_o|$; $R_w = [\Sigma w(|F_o| - |F_c|)^2 / \Sigma w F_o^2]^{1/2}$.

(iii) **Compound (7).** Data were collected for a yellow plate-like crystal mounted on top of a glass fiber. Unit cell parameters were determined from a least-square treatment of the SET4 setting angles of 25 reflections in the range $8.00 < 2\theta < 18.0^\circ$. The intensities of 6166 reflections were corrected for Lp effects, absorption (DIFABS²¹, correction range 0.56 – 1.00), extinction (coefficient = 6.68310×10^{-7}) and crystal decay (9.5%). In the final cycle of full-matrix least-squares all non-hydrogen atoms were refined anisotropically. All hydrogen atoms were added to the respective carbon atoms at calculated positions (C–H: phenyl and methyl distances 1.08 and 0.97 Å) but not refined. The remaining maximum and minimum electron density features in the final difference Fourier map are equal to 0.20 and $-0.20 \text{ e}/\text{\AA}^3$, respectively.

(iv) **Compound (9).** Data were collected at 15 °C for a colorless prismatic crystal mounted on top of a glass fiber and employing a Rigaku RAXIS II imaging plate area detector. Unit cell parameters were determined from a least-square treatment of 30 reflections. The intensities of 2190 reflections were corrected for Lp effects and secondary extinction (coefficient = 3.48676×10^{-6}). In the final cycle of full-matrix least-squares all non-hydrogen atoms were refined anisotropically. All hydrogen atoms were added to the respective carbon atoms at calculated positions (C–H: phenyl and methyl distances 1.08 and 0.97 Å) but not refined. The remaining maximum and minimum electron density features in the final difference Fourier map are equal to 0.20 and $-0.22 \text{ e}/\text{\AA}^3$, respectively.

ACKNOWLEDGMENTS

This work was supported by the Ministry of Education, Science, Sports and Culture, Japan [Grant-in-Aid for Scientific Research (A): Grant No. 07404035 and Grant-in-Aid for Encouragement of Young Scientists: Grant No. 08740484], and the Fund of Tsukuba Advanced Research Alliance (TARA) project [University of Tsukuba].

Supplementary Material Available

Detailed crystallographic data, positional and thermal parameters, and bond distances and angles have been deposited (73 pages). The procedure for ordering information is given on any current masthead page.

REFERENCES

1. D. Mansuy, P. Valadon, I. Erdelmeier, P. Lopez-Garcia, C. Amar, J. P. Girault, and P. M. Dansette, *J. Am. Chem. Soc.*, 1991, **113**, 7825; P. M. Dansette, T. Do Cao, H. El Amri, and D. Mansuy,

- Biochem. Biophys. Res. Commun.*, 1992, **186**, 1624; P. Lopez-Garcia, P. M. Dansette, P. Valadon, C. Amar, P. Beaune, F. Guengerich, and D. Mansuy, *Eur. J. Biochem.*, 1993, **213**, 223; P. Lopez-Garcia, P. Dansette, and D. Mansuy, *Biochemistry*, 1994, **33**, 166; A. Treiber, P.M. Dansette, H. El Amri, J. -P. Girault, D. Ginderow, J. -P. Mornon, and D. Mansuy, *J. Am. Chem. Soc.*, 1997, **119**, 1565.
2. W. L. Mock, *J. Am. Chem. Soc.*, 1970, **92**, 7610.
 3. A. E. Skaugset, T. B. Rauchfuss, and C. L. Stern, *J. Am. Chem. Soc.*, 1990, **112**, 2432; P. J. Fagan and W. A. Nugent, *J. Am. Chem. Soc.*, 1988, **110**, 2310.
 4. N. Furukawa, H. Hoshiai, T. Shibutani, M. Higaki, F. Iwasaki, and H. Fujihara, *Heterocycles*, 1992, **34**, 1085; References are cited therein.
 5. N. Furukawa, S-Z. Zhang, S. Sato, and M. Higaki, *Heterocycles*, 1997, **44**, 61.
 6. Y. Li, M. Matsuda, T. Thiemann, T. Sawada, S. Mataka, and M. Thashiro, *Synlett*, **1996**, 461.
 7. K. Torssell, *Acta Chem. Scand.*, 1970, **B30**, 353; J. Bailey and E. W. Cummins, *J. Am. Chem. Soc.*, 1954, **76**, 1936; A. M. Neperstkov, J. B. Macaulay, M. J. Newlands, and A. G. Fallis, *Tetrahedron Lett.*, 1989, **38**, 5077.
 8. P. Pouzet, I. Erdelmeier, D. Ginderow, J. -P. Mornon, P. Dansette, and D. Mansuy, *J. Chem. Soc., Chem. Commun.*, 1995, 473.
 9. P. C. Hariharan and J. A. Pople, *Theor. Chim. Acta*, 1973, **28**, 213; M. M. Francl, W. J. Pietro, W. J. Hehre, J. S. Binkley, M. S. Gordon, D. J. DeFrees, and J. A. Pople, *J. Chem. Phys.*, 1982, **77**, 3654.
 10. *Spartan* version 4.1, Wavefunction, Inc., Irvine, CA, 1995.
 11. *Gaussian 94* (Revision D.2), M. J. Frisch, G. W. Trucks, H. B. Schlegel, P. M. W. Gill, B. G. Johnson, M. A. Robb, J. R. Cheeseman, T. A. Keith, G. A. Petersson, J. A. Montgomery, K. Raghavachari, M. A. Al-Laham, V. G. Zakrzewski, J. V. Ortiz, J. B. Foresman, J. Cioslowski, B. B. Stefanov, A. Nanayakkara, M. Challacombe, C. Y. Peng, P. Y. Ayala, W. Chen, M. W. Wong, J. L. Andres, E. S. Replogle, R. Gomperts, R. L. Martin, D. J. Fox, J. S. Binkley, D. J. Defrees, J. Baker, J. P. Stewart, M. Head-Gordon, C. Gonzalez, and J. A. Pople, Gaussian, Inc., Pittsburgh, PA, 1995.
 12. E. Goldstein, B. Beno, and K. N. Houk, *J. Am. Chem. Soc.*, 1996, **118**, 6036.
 13. N. H. Werstiuk and J. Ma, *Can. J. Chem.*, 1994, **72**, 2493.

14. S. Inagaki, H. Fujimoto, and K. Fukui, *J. Am. Chem. Soc.*, 1976, **98**, 4054; M. Ishida, T. Aoyama, Y. Beniya, S. Yamabe, S. Kato, and S. Inagaki, *Bull. Chem. Soc. Jpn.*, 1993, **66**, 3430.
15. A. Altomare, M. C. Burla, M. Camalli, M. Cascarano, C. Giacovazzo, A. Guagliardi, and G. Polidori, SIR92, *J. Appl. Cryst.*, (submitted 1995).
16. D. H. Flank, *Acta Crystallogr.*, 1983, **A39**, 876.
17. D. T. Cromer and J. T. Waber, "*International Tables for X-Ray Crystallography*", Vol. **IV**, The Kynoch Press, Birmingham, England, Table 2.2B, 1974.
18. J. A. Ibers and W. C. Hamilton, *Acta Crystallogr.*, 1964, **17**, 781.
19. D. C. Creagh and W. J. McAuley, "*International Tables for X-Ray Crystallography*", Vol. **C**, Kluwer Academic Publishers, Boston, Table 4.2.6.8, 219, 1992.
20. teXsan: Crystal Structure Analysis Package, Molecular Structure Corporation (1985 & 1992).
21. DIFABS: N. Walker and D. Stuart, *Acta Cryst.*, 1983, **A39**, 158–166. An empirical absorption correction program.

Received, 2nd June, 1997